Applied Physics Letters

Heteroepitaxially enhanced magnetic anisotropy in $BaTiO_3-CoFe_2O_4$ nanostructures

Cite as: Appl. Phys. Lett. **90**, 113113 (2007); https://doi.org/10.1063/1.2713131
Submitted: 14 December 2006 . Accepted: 07 February 2007 . Published Online: 14 March 2007

Haimei Zheng, Jens Kreisel, Ying-Hao Chu, R. Ramesh, and Lourdes Salamanca-Riba

Heteroepitaxially enhanced magnetic anisotropy in $BaTiO_3$–$CoFe_2O_4$ nanostructures

Haimei Zheng[a)]
Department of Materials Science and Engineering, University of California at Berkeley, Berkeley, California 94720 and Department of Physics, University of California at Berkeley, Berkeley, California 94720

Jens Kreisel
Laboratoire Matériaux et Génie Physique, CNRS, Grenoble Institut of Technologie (INPG), Minatec, 38016 Grenoble, France

Ying-Hao Chu and R. Ramesh[b)]
Department of Materials Science and Engineering, University of California at Berkeley, Berkeley, California 94720 and Department of Physics, University of California at Berkeley, Berkeley, California 94720

Lourdes Salamanca-Riba
Department of Materials Science and Engineering, University of Maryland, College Park, Maryland 30742

(Received 14 December 2006; accepted 7 February 2007; published online 14 March 2007)

The authors have studied the magnetic properties of $BaTiO_3$–$CoFe_2O_4$ nanostructures, which were prepared using pulsed laser deposition. Such nanostructures show a large uniaxial magnetic anisotropy with an easy axis along the pillar long direction. As the growth temperature decreases, the magnetic anisotropy increases. Careful analyses reveal that heteroepitaxial strain is the primary contribution to the magnetic anisotropy. © *2007 American Institute of Physics*.
[DOI: 10.1063/1.2713131]

Materials that possess more than one order parameter simultaneously, i.e., ferroelectricity, ferromagnetism, or ferroelasticity, have attracted considerable interest[1–4] because of their rich coupled phenomena and potential applications in electronic devices. Nanostructures with ferrimagnetic $CoFe_2O_4$ nanopillars heteroepitaxially embedded in a ferroelectric matrix have recently been synthesized.[1,5] Such nanostructures show significant coupling between ferroelectricity and magnetism. The coupling between the ferromagnetic and ferroelectric order parameters is mediated by an elastic strain between the two phases. For example, when an electric field is applied to the nanostructures, strain created by the piezoelectric matrix couples to the magnetostrictive $CoFe_2O_4$ pillars and induces magnetization changes in the $CoFe_2O_4$ phase. Such changes in the magnetization of $CoFe_2O_4$ pillars, and hence the strength of coupling between the ferroelectricity and magnetism, are critically dependent on the magnetic anisotropy and crystalline structure of the nanopillars. In this letter, we report on the structural dependence of magnetic anisotropy of the $BaTiO_3$–$CoFe_2O_4$ nanostructures.

In a bulk magnetic material, magnetocrystalline anisotropy occurs due to the spin-orbit interaction,[6] which is related to the symmetry of the lattice. In nanostructured materials, however, magnetic anisotropy also depends on the shape of the nanomagnet, elastic strain, and other extrinsic effects,[7] such as surface and interface effects,[8,9] interactions between the nanomagnets,[10–12] etc. In $BaTiO_3$–$CoFe_2O_4$ nanostructures, heteroepitaxial strain arises during the growth of the nanostructures due to the lattice mismatch of $CoFe_2O_4$ nanopillars with the substrate and with the $BaTiO_3$ matrix. Since $CoFe_2O_4$ has a significantly large magnetostriction, we believe that the heteroepitaxial strain plays a primary role in the magnetic anisotropy of the $BaTiO_3$–$CoFe_2O_4$ nanostructures.

Figure 1 shows the x-ray diffraction (XRD) θ-2θ spectra obtained from the nanostructures grown at 700, 800, 850, and 900 °C. All the films that were compared have the same film thickness of 400 nm. The XRD spectrum of the sample grown at 700 °C shows a single perovskite phase. Further transmission electron microscopy (TEM) studies indicated that the film has a supersaturated $BaTiO_3$ phase and is het-

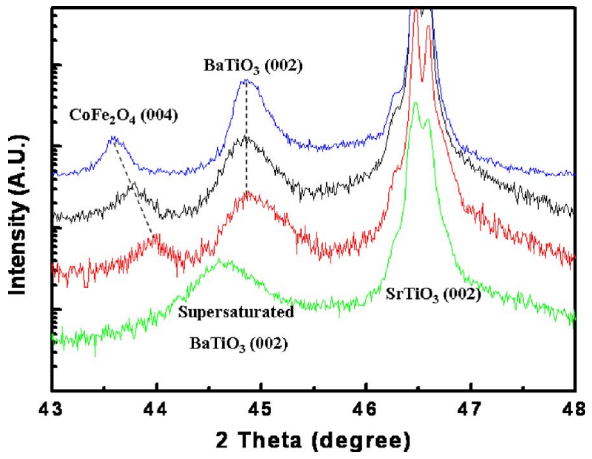

FIG. 1. (Color online) X-ray diffraction θ-2θ spectra obtained from the films grown at temperatures of 700 °C (bottom 1st), 800 °C (bottom 2nd), 850 °C (bottom 3rd), and 900 °C (bottom 4th). Note: The intensity of spectra was plotted in arbitrary units (AU) and the dash lines are guides for the eyes.

[a)]Author to whom correspondence should be addressed; present address: NCEM, Materials Sciences Division, Lawrence Berkeley National Laboratory, Berkeley, CA 94720; electronic mail: haimei@berkeley.edu
[b)]Electronic mail: rramesh@berkeley.edu

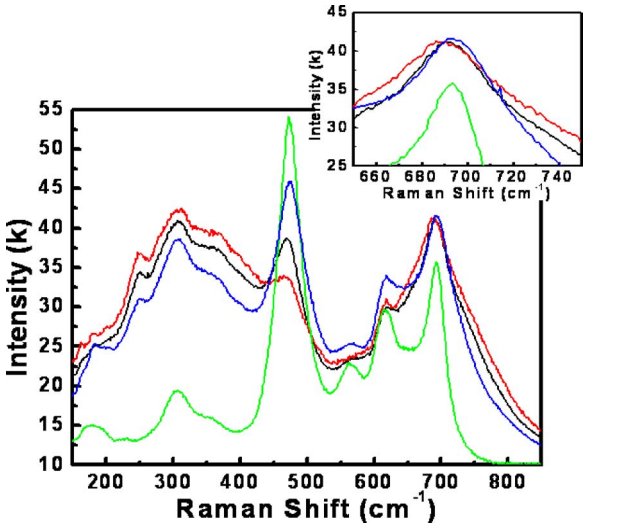

FIG. 2. (Color online) Raman spectra obtained from samples grown at 800 °C (top 1st), 850 °C (top 2nd), and 900 °C (top 3rd) and $CoFe_2O_4$ spectrum (top 4th) for comparison.

eroepitaxial with the substrate. No nanopillar type of structure was observed in these films. We believe that the lack of phase separation at low growth temperature is due to the kinetic limitation. For the films grown at 800 °C and above, we observe $CoFe_2O_4$ nanopillars heteroepitaxially embedded in a $BaTiO_3$ matrix (detailed three-dimensional growth has been reported earlier[13]). The $CoFe_2O_4$ pillars are compressively strained out of plane, and this strain increases as the growth temperature decreases. This is indicated by a systematical shift of the $CoFe_2O_4$ (004) spectrum to a higher angle as the growth temperature decreases. We also observed that the peak position of $BaTiO_3$ matrix remains essentially the same (with negligible strain) for all the films. We believe that this compressive strain in the $CoFe_2O_4$ nanopillars is induced by the lattice mismatch with the $BaTiO_3$ matrix and not from the $SrTiO_3$ substrate. A heteroepitaxy induced tensile strain along $CoFe_2O_4$ nanopillars is expected for a heteroepitaxial film on the $SrTiO_3$, since the unit cell of $SrTiO_3$ (a =3.91 Å) is smaller than a half unit cell of $CoFe_2O_4$ (a=8.38 Å). However, such strain should be relaxed in a film with thickness of 400 nm. In addition, we have found that $CoFe_2O_4$ nanopillars in a $BaTiO_3$ matrix grown on MgO (a=4.23 Å) substrate are also under out-of-plane compressive strain, further confirming that the origin of the strain is from the constraint that is imposed by the $BaTiO_3$ matrix and not from the substrate.

Concurrently, TEM observations confirm that the average diameter of the nanopillars decreases with decreasing deposition temperature. The lateral size of the $CoFe_2O_4$ pillars decreases from about 70 nm in films grown at 950 °C to about 9 nm in films grown at 750 °C. The separation between the pillars also decreases at lower growth temperature. A lower density of dislocations was observed at the interface in films grown at lower growth temperature than at higher growth temperature, which suggests that the lattice-mismatch-induced strain is relaxed by forming dislocations at the interface.

The heteroepitaxial strain (specifically, the in-plane strain) in the nanostructures was further studied by Raman spectroscopy. Figure 2 presents Raman spectra for samples grown at 800, 850, and 900 °C and, for comparison, a spectrum of a 400 nm thick relaxed $CoFe_2O_4$ film. The results can be summarized as follows: (i) The signal from the nanostructures is dominated by Raman scattering from the $CoFe_2O_4$ pillars, due to the intrinsically lower Raman scattering of $BaTiO_3$. (ii) The spectral fingerprint of the pillars is similar to the $CoFe_2O_4$ thin film reference data and bulk data from literature,[14] suggesting that the pillars adopt the bulk crystal structure. The differences in the spectra between nanostructures and the thick $CoFe_2O_4$ reference film are due to scattering from the $SrTiO_3$ substrate. (iii) A closer inspection of the thin film spectra shows that most Raman bands present a low-wave-number shift when going from the 900 to the 800 °C sample. The inset of Fig. 2 illustrates a shift of $\approx$6 cm^{-1} towards lower wave numbers for the strong band at 795 cm^{-1}. Such strain-induced band shifts are consistent with the above-described changes in the XRD data. As it was reported for perovskite films,[15–17] Raman scattering is characteristic of the in-plane tensile strain, while the XRD data in Fig. 1 characterize the out-of plane compressive strain. In order to estimate the induced strain, we can use Raman data from hydrostatic pressure experiments, which are available in the literature for $CoFe_2O_4$.[14] Hydrostatic pressure experiments, of course, cannot truly monitor biaxial strain in thin films; nevertheless, it has been shown in literature that it can be used to provide a reasonable estimate of the strain state.[15–17] On the basis of this hypothesis, the high-pressure data allow the identification of the strain in the thin $CoFe_2O_4$ pillars of the 800 °C film as a tensile strain, with respect to bulk $CoFe_2O_4$, of roughly 2 GPa (the 795 cm^{-1} band with a Grüneisen parameter γ=0.41 shifts at a rate of 3 cm^{-1}/GPa).[14] Finally, we note the Raman bands of the 800 °C film present a larger linewidth than the other films, which we attribute to a decreasing coherence length with decreasing lateral size of the pillars.

Figure 3(a) shows the in-plane (with the applied magnetic field along the [100] direction) and out-of-plane (magnetic field along the [001] direction) magnetization (M) versus field (H) loops of the nanostructures grown at 900 °C. The magnetization was normalized to the volume fraction of $CoFe_2O_4$ (35%). A large uniaxial magnetic anisotropy with an easy axis along the [001] direction of the films is observed. A linear extrapolation of the in-plane magnetic loop yields an anisotropy field of about 51 kOe. In order to explore the origin of the large magnetic anisotropy of the embedded $CoFe_2O_4$ pillars, several factors were considered. Firstly, the magnetocrystalline anisotropy is neglected between the [001] and [100] directions of $CoFe_2O_4$. Secondly, we calculated the shape anisotropy contribution for the $CoFe_2O_4$ nanopillars. Since they have a typical aspect ratio of about 10, the demagnetization factor[18,19] for a cylinder with aspect ratio of 10 is N_z=0.0172. The associated anisotropy energy density is $E_{\text{shape}}=2\pi(N_x-N_z)M_s^2$, where $N_x=(1-N_z)/2$. For a saturation magnetization (M_s) of 360 emu/cm^3, the shape anisotropy field is calculated to be $H_{\text{shape}}=2E_{\text{shape}}/M_s=2.0$ kOe, which is much smaller than the experimentally observed value. Thirdly, the heteroepitaxial strain in the $CoFe_2O_4$ lattice contributes to the magnetic anisotropy through magnetostriction and gives rise to magnetoelastic energy as calculated below. For the film grown at 900 °C, since a compressive strain along the [001] direction (ε_{001}) of the $CoFe_2O_4$ pillars is about $\varepsilon_{001}=-1.1\%$, the magnetoelastic energy density associated with this stress is $e=-3\lambda_{001}\sigma_{001}/2=-3\lambda_{001}Y\varepsilon_{001}/2=7.88\times10^6$ erg/cm^3,

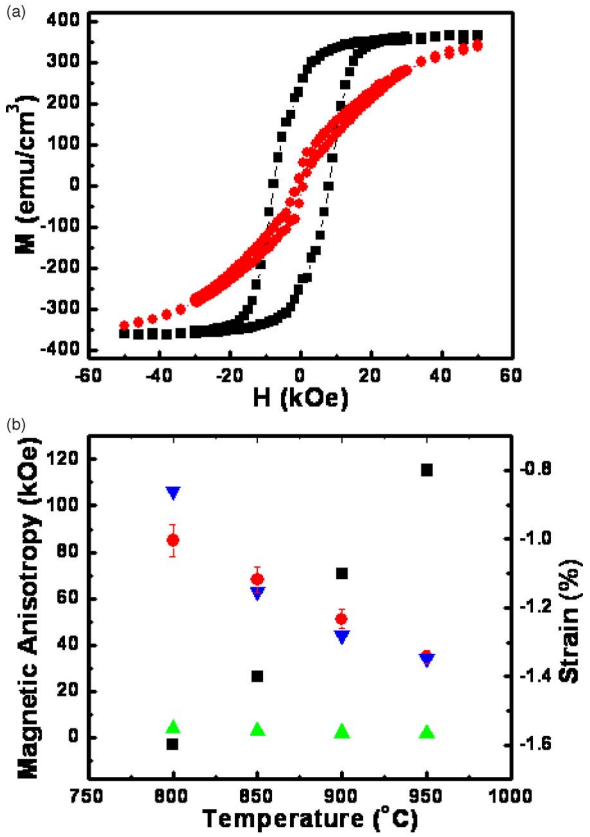

FIG. 3. (Color online) (a) Out-of-plane [001] (■) and in-plane [100] (●) magnetic hysteresis loops from a $BaTiO_3$–$CoFe_2O_4$ nanostructure thin film grown at 900 °C. (b) Heteroepitaxial strain (■) and magnetic anisotropy [experimental (●), stress induced anisotropy (▼), and shape anisotropy (▲)] of the films grown at various temperatures.

where λ_{001} is the magnetostriction coefficient of $CoFe_2O_4$ (taken to be $\lambda_{001} \sim -350 \times 10^{-6}$) and Y is Young's modulus (141.6 GPa).[20] An anisotropy field of $H_{stress}=2e/M_s$ =44 kOe was obtained. A total estimated anisotropy (H_{stress} $+H_{shape}$) is of about 46 kOe, which is comparable to our experimentally observed value of 51 kOe.

We observed an increase in this magnetic anisotropy as the growth temperature decreases. Similar calculations on magnetic anisotropy using the compressive strain obtained from XRD have been carried out. Figure 3(b) shows the calculated stress anisotropy, shape anisotropy, and experimentally observed values of magnetic anisotropy for the films grown at 800, 850, 900, and 950 °C, illustrating that the heteroepitaxial strain-induced anisotropy is the main contribution to the experimentally measured magnetic anisotropy. The discrepancy between the calculated and experimental values for the anisotropy field of the film grown at 800 °C may be induced by the linear extrapolation of the experimental value and/or more complex phenomena due to the smaller spacing between the pillars, such as dipolar interactions among the $CoFe_2O_4$ pillars, etc. We point out that the magnetic properties of the nanostructures are highly dependent on their structures. In this study, $BaTiO_3$–$CoFe_2O_4$ nanostructures grown at different temperatures were carefully selected to make sure that they have the same film thickness, similar shape of nanopillars, and three-dimensional heteroepitaxial features. The magnetic behavior of the thin films with a supersaturated phase is dramatically different. It shows a considerably suppressed magnetization and an in-plane anisotropy, which is not compared with the nanostructures.

In summary, $BaTiO_3$–$CoFe_2O_4$ nanostructures show a large uniaxial anisotropy with an easy axis along the film growth direction. There is a systematic increase of strain in $CoFe_2O_4$ pillars and an increase of magnetic anisotropy when the growth temperature of the nanostructure decreases. We believe that the heteroepitaxial induced anisotropy is the main contribution to the large anisotropy field. A detailed study on the effect of magnetic anisotropy on the strength of magnetoelectric coupling is of great value to further explore the multiferroic nanostructures.

The authors would like to thank Y. Suzuki, Y. Takamura, and R. V. Chopdekar at UC Berkeley for useful discussions. This project was initially started at NSF-MRSEC of the University of Maryland under Contract No. DMR-00-80008. Currently, this work is supported by an ONR MURI program under Contract No. E-21-6RU-G4 at the UC Berkeley. The authors acknowledge support of NCEM, Lawrence Berkeley National Laboratory. One of the authors (J.K.) acknowledges financial support from the French Research Agency (ANR).

[1] H. Zheng, J. Wang, S. E. Lofland, Z. Ma, L. Mohaddes-Ardabili, T. Zhao, L. Salamanca-Riba, S. R. Shinde, S. B. Ogale, F. Bai, D. Viehland, Y. Jia, D. G. Schlom, M. Wuttig, A. Roytburd, and R. Ramesh, Science **303**, 661 (2004).
[2] C. W. Nan, G. Liu, Y. H. Lin, and H. D. Chen, Phys. Rev. Lett. **94**, 197203 (2005).
[3] I. Levin, J. H. Li, J. Slutsker, and A. L. Roytburd, Adv. Mater. (Weinheim, Ger.) **18**, 2044 (2006).
[4] C. Ederer and N. A. Spaldin, Curr. Opin. Solid State Mater. Sci. **9**, 128 (2006).
[5] F. Zavaliche, H. Zheng, L. Mohaddes-Ardabili, S. Y. Yang, Q. Zhan, P. Shafer, E. Reilly, R. Chopdekar, Y. Jia, P. Wright, D. G. Schlom, Y. Suzuki, and R. Ramesh, Nano Lett. **5**, 1793 (2005).
[6] D. Wang, R. Wu, and A. J. Freeman, Phys. Rev. Lett. **70**, 869 (1993).
[7] Y. Suzuki, G. Hu, R. B. van Dover, and R. J. Cava, J. Magn. Magn. Mater. **191**, 1 (1999).
[8] R. H. Kodama, J. Magn. Magn. Mater. **200**, 359 (1999).
[9] R. H. Kodama, A. E. Berkowitz, E. J. McNiff, Jr., and S. Foner, Phys. Rev. Lett. **77**, 394 (1996).
[10] B. Hillebrands, C. Mathieu, C. Hartmann, M. Bauer, O. Büttner, S. Riedling, B. Roos, S. O. Demokritov, B. Bartenlian, C. Chappert, D. Decanini, F. Rousseaux, E. Cambril, A. Müller, B. Hoffmann, and U. Hartmann, J. Magn. Magn. Mater. **175**, 10 (1997).
[11] R. P. Cowburn, D. K. Koltsov, A. O. Adeyeye, and M. E. Welland, Europhys. Lett. **48**, 221 (1999).
[12] C. Mathieu, C. Hartman, M. Bauer, O. Büttner, S. Riedling, B. Ross, S. O. Demokritov, B. Hillebrands, B. Bartenlian, C. Chappert, D. Decanini, F. Rousseaux, E. Cambril, A. Müller, B. Hoffmann, and U. Hartmann, Appl. Phys. Lett. **70**, 2912 (1997).
[13] H. Zheng, J. Wang, L. Mohaddes-Ardabili, D. G. Schlom, M. Wuttig, L. Salamanca-Riba, and R. Ramesh, Appl. Phys. Lett. **85**, 2035 (2004).
[14] Z. Wang, R. T. Downs, V. Pischedda, R. Shetty, S. K. Saxena, C. S. Zha, Y. S. Zhao, D. Schiferl, and A. Waskowska, Phys. Rev. B **69**, 094101 (2003).
[15] P. S. Dobal and R. S. Katiyar, J. Raman Spectrosc. **33**, 405 (2002).
[16] E. Ching-Prado, A. Reynés-Figueroa, R. S. Katiyar, S. B. Majumder, and D. C. Agrawal, J. Appl. Phys. **78**, 1920 (1995).
[17] J. A. Sanjurjo, E. Lopez-Cruz, and G. Burns, Phys. Rev. B **28**, 7260 (1983).
[18] R. M. Bozorth, Ferromagnetism (IEEE, Piscataway, NJ, 1993).
[19] *Magnetic Oxides and Related Compounds*, Landolt-Börnstein, New Series, Group III, Vol. 4, Pt. B (Springer, Berlin, 1970), pp. 366–393.
[20] *Ferromagnetism*, edited by S. Flügge (Springer, Berlin, 1966), Vol. 18:2, p. 452.